A High-Energy Charge-Separated State of 1.70 eV from a High-Potential Donor–Acceptor Dyad: A Catalyst for Energy-Demanding Photochemical Reactions

Gary N. Lim, Christopher O. Obondi, and Francis D'Souza*

Abstract: *A high potential donor–acceptor dyad composed of zinc porphyrin bearing three meso-pentafluorophenyl substituents covalently linked to C_{60}, as a novel dyad capable of generating charge-separated states of high energy (potential) has been developed. The calculated energy of the charge-separated state was found to be 1.70 eV, the highest reported for a covalently linked porphyrin–fullerene dyad. Intramolecular photoinduced electron transfer leading to charge-separated states of appreciable lifetimes in polar and nonpolar solvents has been established from studies involving femto- to nanosecond transient absorption techniques. The high energy stored in the form of charge-separated states along with its persistence of about 50–60 ns makes this dyad a potential electron-transporting catalyst to carry out energy-demanding photochemical reactions. This type of high-energy harvesting dyad is expected to open new research in the areas of artificial photosynthesis especially producing energy (potential) demanding light-to-fuel products.*

Artificial photosynthesis holds great promise to meet the growing energy needs by providing renewable solar energy and fuels.[1–7] Elegantly designed multi-modular donor—acceptor systems capable of producing charge-separated states upon photoexcitation are key in building energy-harvesting devices. The stored energy in the charge-separated species (electrochemical potential) could be used to produce solar fuels in a catalytic fashion. This process is analogous to natural photosynthesis in which the chemical energy produced via *trans*-membrane charge separation via a multistep electron-transfer process is converted into other forms of biologically useful energy stored in the chemical bonds of the products.[8] Two factors mandate the applicability of the charge-separated states for their catalytic applications, these are, their persistence prior to the relaxation to the ground state (lifetime of charge-separated states) and the amount of stored energy as electrochemical potential. Often, using the concept of electron/hole migration in well-designed multi-

modular donor–acceptor systems, long-lived charge-separated states have been achieved, however, at the cost of lowering the energy of the charge-separated states due to the energy loss encountered during the processes of sequential electron-transfer events.[1–3] Such charge-separated states although long-living may not carry enough energy (potential) to perform fuel-producing chemical reactions, for example, oxidation of water to produce protons. Consequently, there is a great need for donor–acceptor systems capable of generating high-energy charge-separated states with appreciable lifetimes.

Herein, we have synthesized a donor–acceptor dyad using a difficult to oxidize electron donor, that is, zinc porphyrin having pentafluorophenyl substituents and fullerene, C_{60} as the acceptor (Figure 1). Fullerene owing to its favorable
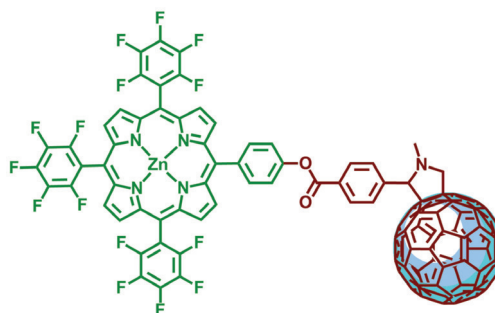

Figure 1. Structure of the high potential zinc porphyrin–fullerene dyad developed to generate high-energy charge-separated states.

reduction potential and low reorganization-energy demand is a preferred choice of an electron acceptor.[9] As shown herein, owing to the presence of fluorine substituents, zinc porphyrin $((F_{15}P)Zn)$ oxidation becomes harder by 430 mV compared to the traditionally used zinc porphyrin,[10] however, without drastically compromising its spectral (absorption and emission) properties. The constructed energy level diagram shows that photoinduced electron transfer from the $^1(F_{15}P)Zn^*$ to fullerene is indeed possible to yield high energy charge-separated states. The calculated energy of the charge-separated state was as high as 1.70 eV enough to drive most of the catalytic processes (for example, water oxidation potential is 1.23 V). Evidence for the formation of such high-energy charge-separated state and kinetics of forward and reverse charge-separation processes have been secured from studies involving transient absorption studies ranging from femto- to nanosecond timescales.

[*] G. N. Lim, C. O. Obondi, Prof. Dr. F. D'Souza
Department of Chemistry
University of North Texas
1155 Union Circle, #305070, Denton, TX 76203-5017 (USA)
E-mail: Francis.DSouza@UNT.edu

Synthesis of the $(F_{15}P)Zn\text{-}C_{60}$ was accomplished according to Scheme S1 in the Supporting Information. This involved first synthesis of *meso*-tris(pentafluorophenyl)-(4-hydroxy-phenyl)-porphyrin. This compound was subsequently reacted with 4-carboxy benzaldehyde to obtain *meso*-tris(pentafluorophenyl)-(4′-formylphenyl benzoate)porphyrin. Reaction of formyl functionalized porphyrin with C_{60} and sarcosine according to Prato's reaction yielded the free-base porphyrin $(F_{15}P)\text{–}C_{60}$ dyad. The free-base porphyrin was subsequently metallated using zinc acetate to obtain $(F_{15}P)Zn\text{–}C_{60}$ dyad. The purity of the compound was checked by running thin-layer chromatography, and the structural identity was established from ^1H and ^{13}C NMR spectroscopy and MALDI-mass spectrometry techniques. The dyad was stored in dark prior to performing photochemical studies.

Figure 2 a,b show the absorption and fluorescence spectra of the dyad along with the control compounds, $(F_{15}P)Zn$ and fulleropyrrolidine, in benzonitrile. The absorption spectral pattern of porphyrin was typical of that of metalloporphyrin, however, the peak maxima were red-shifted by 4–5 nm compared with tetraphenylporphyrin due to the presence of electron-withdrawing fluoro substituents on the phenyl rings. Covalent attachment of C_{60} had virtually no effect, meaning absence of appreciable intramolecular interactions between them. The fluorescence spectrum of the control $(F_{15}P)Zn$ revealed two bands at $\lambda = 600$ and 650 nm which were quenched by 46 % in benzonitrile and 38 % in toluene for the $(F_{15}P)Zn\text{–}C_{60}$ dyad suggesting the occurrence of excited state events in the dyad. Scanning the wavelength into the $^1C_{60}*$ emission range of 720 nm revealed no emission of C_{60} suggesting absence of singlet–singlet energy transfer from the excited $^1(F_{15}P)Zn*$ to C_{60}. This is conceivable since fulleropyrrolidine virtually had no absorbance in the 575–675 nm range where $^1(F_{15}P)Zn*$ fluoresce.

To ascertain that the quenching is due to processes originated from the singlet excited porphyrin and not static (lowering lifetime due to ground state complex formation), fluorescence lifetimes were measured for the control and the dyad. The decay profiles could be fitted satisfactorily to a monoexponential decay function ($\chi^2 < 1.2$) in all of the cases (see Figure 2 c for decay curves and fits). The lifetime of the $(F_{15}P)Zn$ control was found to be 1.67 and 1.83 ns, respectively, in benzonitrile and toluene. For the $(F_{15}P)Zn\text{–}C_{60}$ dyad, these lifetimes were found to be 0.76 and 0.82 ns, respectively. The lowering of the lifetime of $^1(F_{15}P)Zn*$ in the dyad shows the occurrence of excited state events in both solvents.[11]

It was also important to evaluate the triplet energy level of $(F_{15}P)Zn$. The phosphorescence spectrum of $(F_{15}P)Zn$ recorded in methyl cyclohexane containing 5 % CH_3I at liquid nitrogen temperature revealed a peak at 758 nm (Figure 2 d). This resulted in E_T value for $^3[(F_{15}P)Zn]*$ of
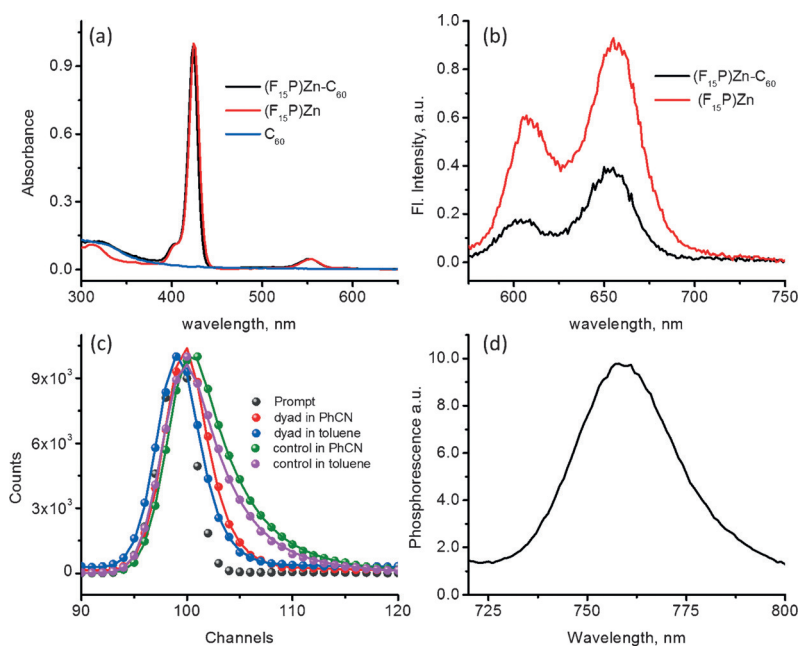

Figure 2. a) Optical absorbance and b) steady-state fluorescence spectra ($\lambda_{ex} = 552$ nm) of the indicated compounds in benzonitrile at room temperature. c) Time-resolved emission spectra of indicated compounds monitored at porphyrin emission wavelength. Control $= (F_{15}P)Zn$, prompt $=$ light scatter. The decay curve fits are shown in solid lines. d) Phosphorescence spectrum of $(F_{15}P)Zn$ control in methyl cyclohexane containing 5 % CH_3I at liquid-nitrogen temperature.

1.64 eV. This value compares with a E_T value for $^3C_{60}*$ of 1.55 eV.

The differential pulse voltammogram (DPV) of the dyad in benzonitrile is shown in Figure 3. Well defined redox waves corresponding to both oxidation and reduction were observed. The first two oxidation processes corresponding to the $(F_{15}P)Zn^{\cdot+}$ and $(F_{15}P)Zn^{2+}$ formation were located at 0.71 and 0.95 V vs. Fc/Fc^+, respectively, while the first reduction corresponding to the $(F_{15}P)Zn^{\cdot-}$ formation was located at -1.77 V vs. Fc/Fc^+. The fulleropyrrolidine in the dyad revealed the first three reductions at -1.01, -1.40, and -1.97 V vs. Fc/Fc^+. There was no appreciable shift in the redox potentials of the dyad when compared to that of the corresponding control compounds suggesting lack of ground state interactions between the entities. Importantly, the
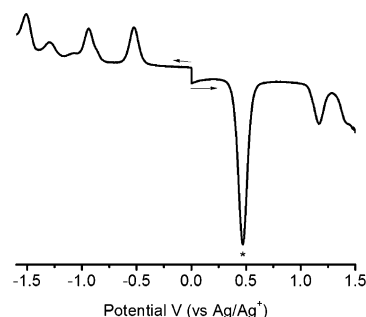

Figure 3. DPVs of the $(F_{15}P)Zn\text{–}C_{60}$ dyad in benzonitrile, 0.1 M (n-$Bu_4N)ClO_4$. Scan rate $= 5$ mV s^{-1}, pulse width $= 0.25$ s, pulse height $= 0.025$ V. The oxidation wave of ferrocene (Fc/Fc^+) used as the internal reference is shown with an asterisk.

430 mV anodic shift of the first oxidation of $(F_{15}P)Zn$ compared to $(TPP)Zn$ ($TPP =$ tetraphenylporphyrin, $E_{1/2} = 0.28$ V vs. Fc/Fc$^+$)[10] is noteworthy.

Using the spectral and electrochemical data, free-energy change associated for charge separation (ΔG_{CS}) and charge recombination (ΔG_{CR}) were calculated according to Rehm and Weller approach.[12,13] From these calculations, ΔG_{CS} and ΔG_{CR} values of -0.34 and -1.70, respectively, in bezonitrile were obtained. Figure 4 shows the energy-level diagram
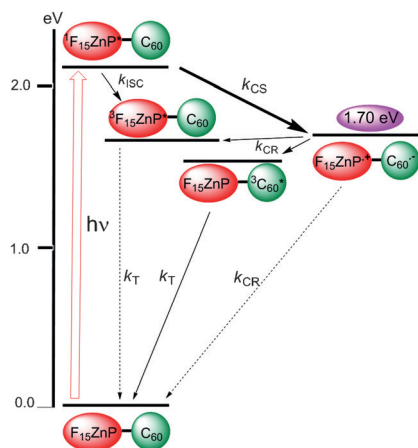

Figure 4. Energy-level diagram depicting the different photochemical events occurring in the $(F_{15}P)Zn–C_{60}$ dyad upon photoexcitation leading to the formation of high-energy charge-separated state. Abbreviations: CS = charge separation, CR = charge recombination, ISC = intersystem crossing, T = triplet emission.

constructed to visualize the different photochemical events. At the excitation wavelength of 400 nm, $(F_{15}P)Zn$ in the dyad is primarily being excited. The $^1(F_{15}P)Zn^*–C_{60}$ thus formed could undergo energy transfer to produce $(F_{15}P)Zn–^1C_{60}^*$ (minor process), or intersystem crossing to produce $^3(F_{15}P)Zn^*–C_{60}$ or electron transfer to yield the high-energy $(F_{15}P)Zn^{•+}–C_{60}^{•-}$ charge-separated state. Importantly, the energy of the charge-separated state in benzonitrile is about 1.70 V, the highest ever for a zinc porphyrin–C_{60} radical ion pair. The recombination mechanism of these possible photoproducts also deserves special mention. The $(F_{15}P)Zn^{•+}–C_{60}^{•-}$ charge-separated state could populate the energetically low lying $^3(F_{15}P)Zn^*$ or $^3C_{60}^*$ states within the dyad prior to its relaxation to the ground state. Interestingly, the $^3(F_{15}P)Zn^*–C_{60}$ formed either via the intersystem crossing from $^1(F_{15}P)Zn^*$ or via charge recombination could undergo triplet–triplet energy transfer to populate $^3C_{60}^*$ within the dyad. Femtosecond transient spectral studies were performed to secure evidence for these processes and also to obtain their kinetic information.

One of the key evidences for the occurrence of charge separation in a donor–acceptor dyad is to detect the transient spectral features corresponding to the products of charge-separated state, that is, $(F_{15}P)Zn^{•+}$ and $C_{60}^{•-}$ species. The $C_{60}^{•-}$ is known for its absorbance in the near-IR region around 1020 nm.[1,2] To seek spectral signature bands of $(F_{15}P)Zn^{•+}$, spectroelectrochemical studies were performed on $(F_{15}P)Zn$

in benzonitrile at an applied potential of 0.80 V vs. Fc/Fc$^+$ corresponding to its first oxidation process. As shown in Figure S1, during this process, both Soret and visible bands located at $\lambda = 425$ and 555 nm revealed diminished intensity accompanied by new peaks at $\lambda = 780$ and 905 nm. Isosbestic points at $\lambda = 398$, 442, 540, and 575 nm were observed. Appearance of transient peaks at these wavelengths would serve as a direct proof for the occurrence of charge separation in the dyad.

Femtosecond differential transient absorption spectroscopic method was utilized to secure evidence for the occurrence of photoinduced charge separation from the excited singlet state of $(F_{15}P)Zn$ in the high potential dyad. First, the $(F_{15}P)Zn$ control compound was recorded in benzonitrile and toluene and the data is shown in Figure S2. The transient spectra of $(F_{15}P)Zn$ in benzonitrile revealed instantaneously formed $^1(F_{15}P)Zn^*$ with positive peaks at 459, 581, 702 and 1290 nm and negative peaks at 555 and 627 nm. The 555 nm peak was due to ground state depletion while the 627 nm peak had contributions from both ground state depletion and stimulated emission. Decay/recovery of the positive/negative peaks resulted in populating the $^3(F_{15}P)Zn^*$ via intersystem crossing with the triplet peaks located at 463, 671 and 848 nm. Similar spectral features were also observed in toluene. The decay profile of the 1290 nm peak, shown as
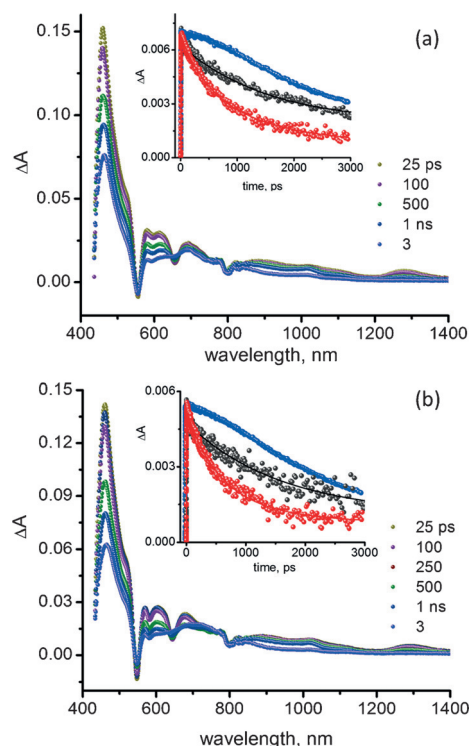

Figure 5. Femtosecond differential transient absorption spectra (400 nm excitation of 100 fs pulses) of $(F_{15}P)Zn–C_{60}$ dyad in Ar-saturated a) benzonitrile and b) toluene at the indicated delay times. Insets show time profile of the 1290 nm peak corresponding singlet excited state of $(F_{15}P)Zn$ control (black line), 1290 nm peak of $(F_{15}P)Zn–C_{60}$ (red), and the 1020 nm peak corresponding to $C_{60}^{•-}$ (blue).

an inset, agreed well with the expected singlet lifetime of the $(F_{15}P)Zn$.

Figure 5 shows the differential transient absorption spectra of the $(F_{15}P)Zn–C_{60}$ dyad in the investigated solvents. The decay of the instantaneously formed $^1(F_{15}P)Zn^*$ was much faster (see Figure 5 insets for decay profiles of the 1290 nm peak of $(F_{15}P)Zn$ (black) and $(F_{15}P)Zn-C_{60}$ (red)). However, the $^1(F_{15}P)Zn^*$ instead of populating the $^3(F_{15}P)Zn^*$ revealed development of transient peaks corresponding to the $(F_{15}P)Zn^{•+}–C_{60}^{•-}$ charge-separated state. That is, broad spectral features of $(F_{15}P)Zn^{•+}$ at 790 and 905 nm, and a peak at 1020 nm corresponding to $C_{60}^{•-}$ (see spectra recorded at 25 ps delay time, Figure 5) thus confirming the occurrence of photoinduced charge separation. The rate constant for charge separation, k_{CS}[14] was evaluated by monitoring decay of the 1290 nm peak as this peak is sufficiently away from other transient peaks.

The k_{CS} thus calculated was found to be $5.7 \times 10^8 \, s^{-1}$ in benzonitrile and $1.7 \times 10^8 \, s^{-1}$ in toluene. The overall k_{CS} is slower compared to the traditionally used $ZnP–C_{60}$ ($k_{CS} \approx 10^9–10^{10} \, s^{-1}$).[1–3] The quantum yield of charge separation, Φ_f[15] was also calculated, and these values were found to be 40% in benzonitrile and 20% in toluene. These values are reasonable considering smaller free-energy change for charge separation and solvent polarity effects. For calculating the rate constant for charge recombination, k_{CR}, the decay of $C_{60}^{•-}$ peak at 1020 nm was monitored. However, as seen from Figure 5 inset (blue trace), the decay lasted beyond the monitoring time window of our femtosecond transient spectrometer in both solvents and thus demanded complimentary nanosecond transient measurements.

To evaluate the lifetime of the final charge-separated state, nanosecond transient spectral measurements were performed. As pointed out earlier, the energy of the charge-separated state in the present study is above that of $^3(F_{15}P)Zn^*$ (1.64 eV) and $^3C_{60}^*$ (1.55 eV) levels. Under these conditions, the process of charge recombination could populate either one of these states. The transient spectra of $^3(F_{15}P)Zn^*$ (see Figure S3) revealed peaks at 466, 732 and 835 nm in benzonitrile and at 462, 718 and 835 nm in toluene. The decay rate constant was found to be $k_T = 3.5 \times 10^3 \, s^{-1}$ in benzonitrile and $1.3 \times 10^4 \, s^{-1}$ in toluene. Triplet fulleropyrrolidine is known to exhibit peaks at 700 and 835(sh) nm.[2] Interestingly, the nanosecond transient spectra of the dyad in benzonitrile resembled largely that of $^3(F_{15}P)Zn^*$, however, with signature peaks corresponding to $(F_{15}P)Zn^{•+}$ and $C_{60}^{•-}$ species (see the spectrum recorded at 28 ns in Figure 6a). These peaks were not present for $^3(F_{15}P)Zn^*$ as seen in Figure S3a. The decay of the radical ion peaks populated the $^3(F_{15}P)Zn^*$, as witnessed by an increase of the triplet peaks. By 70 ns, the peak at 1020 nm of $C_{60}^{•-}$ was completely vanished. The spectra recorded in toluene also revealed bands
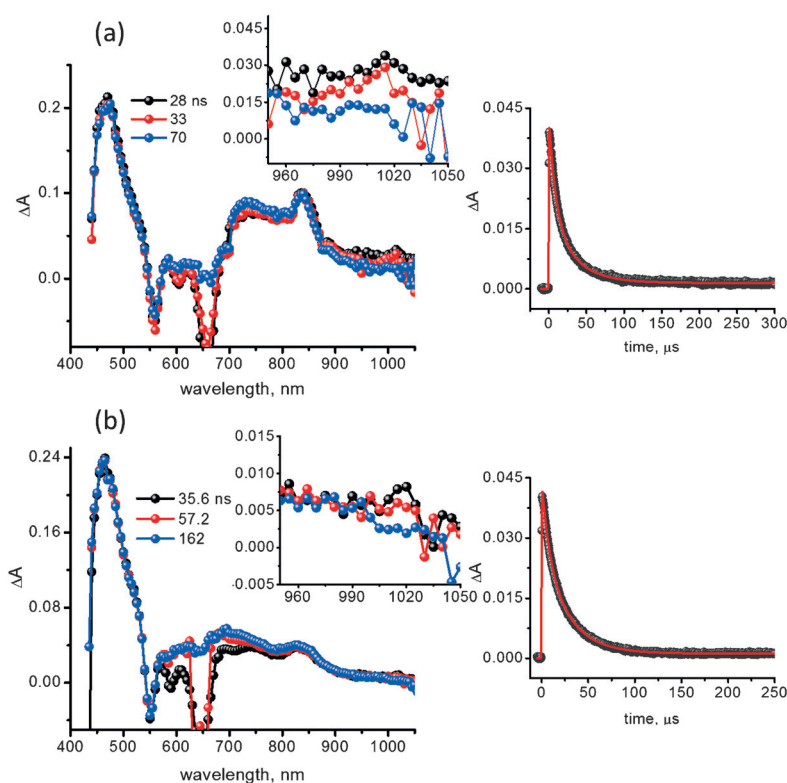

Figure 6. Nanosecond differential transient absorption spectra (425 nm of 8 ns pulses) of $(F_{15}P)Zn–C_{60}$ dyad in Ar-saturated a) benzonitrile and b) toluene at the indicated delay times. Insets show the expanded region of 950–1050 nm revealing the signature peak of $C_{60}^{•-}$. Right hand panel shows the time profile of the 840 nm peak.

corresponding to the charge-separated states (see spectrum recorded at 35 ns delay time in Figure 6b). The weak signal strength of $C_{60}^{•-}$ is conceivable since the quantum yield for charge separation is only 40% and 20% in benzonitrile and toluene, respectively, and by the time the first nanosecond transient spectrum is recorded (ca. 30 ns), most of the radical ion-pair signal originated from the singlet excited $(F_{15}P)Zn$ is depleted due to charge recombination. Under these conditions, it is safer to say that the charge-separated state persists for about 50–60 ns, adequate time to deploy the system for high energy demanding photocatalytic reactions of appropriate energy states. The decay rate constant, k_T of the populated $^3(F_{15}P)Zn^*$ (see Figure 6 right hand panel for the decay curves) was found to be $3.1 \times 10^4 \, s^{-1}$ in benzonitrile and $4.0 \times 10^4 \, s^{-1}$ in toluene.

In summary, the high potential donor–acceptor dyad resulted in high-energy charge-separated state carrying potential of a remarkable 1.70 eV during intramolecular photoinduced electron transfer, the highest for a zinc porphyrin–fullerene dyad reported to date. Coupled with this, and the persistence of the charge-separated state to 50–60 ns makes this dyad an potential photocatalyst to carryout high-energy demanding reactions including light-to-fuel conversion processes. Currently, we are looking into such photocatalytic applications.

[1] a) S. Fukuzumi, K. Ohkubo, T. Suenobu, *Acc. Chem. Res.* **2014**, *47*, 1455–1464; b) S. Fukuzumi, K. Ohkubo, F. D'Souza, J. L. Sessler, *Chem. Commun.* **2012**, *48*, 9801–9815.

[2] a) F. D'Souza, O. Ito, *Chem. Soc. Rev.* **2012**, *41*, 86–96, b) C. B. KC, F. D'Souza, *Coord. Chem. Rev.* **2016**, *322*, 104–141; c) M. El-Khouly, S. Fukuzumi, F. D'Souza, *ChemPhysChem* **2014**, *15*, 30–47.

[3] a) H. Imahori, T. Umeyama, S. Ito, *Acc. Chem. Res.* **2009**, *42*, 1809–1818; b) T. Hasobe, *Phys. Chem. Chem. Phys.* **2010**, *12*, 44–57.

[4] a) N. S. Lewis, D. G. Nocera, *Proc. Natl. Acad. Sci. USA* **2006**, *103*, 15729–15735; b) P. V. Kamat, *J. Phys. Chem. C* **2007**, *111*, 2834–2860.

[5] a) M. R. Wasielewski, *Acc. Chem. Res.* **2009**, *42*, 1910–1921; b) D. Gust, T. A. Moore, A. L. Moore, *Acc. Chem. Res.* **2009**, *42*, 1890–1898.

[6] a) V. Balzani, A Credi, M. Venturi, *ChemSusChem* **2008**, *1*, 26–58; b) G. Ulrich, R. Ziessel, A. Harriman, *Angew. Chem. Int. Ed.* **2008**, *47*, 1184–1201; *Angew. Chem.* **2008**, *120*, 1202–1219; c) E. Schwartz, S. Le Gac, J. J. L. M. Cornelissen, R. J. M. Nolte, A. E. Rowan, *Chem. Soc. Rev.* **2010**, *39*, 1576–1599.

[7] a) D. M. Guldi, A. Rahman, V. Sgobba, C. Ehli, *Chem. Soc. Rev.* **2006**, *35*, 471–487; b) J. N. Clifford, G. Accorsi, F. Cardinali, J. F. Nierengarten, N. Armaroli, *C. R. Chem.* **2006**, *9*, 1005–1013; c) N. Martin, L. Sanchez, M. A. Herranz, B. Illesca, D. M. Guldi, *Acc. Chem. Res.* **2007**, *40*, 1015–1024; d) G. Bottari, G. de la Torre, D. M. Guldi, T. Torres, *Chem. Rev.* **2010**, *110*, 6768–6816; e) D. M. Guldi, V. Sgobba, *Chem. Commun.* **2011**, *47*, 606–610; f) D. González-Rodríguez, E. Carbonell, D. M. Guldi, T. Torres, *Angew. Chem. Int. Ed.* **2009**, *48*, 8032–8036; *Angew. Chem.* **2009**, *121*, 8176–8180.

[8] a) J. S. Connolly, *Photochemical Conversion and Storage of Solar Energy*, Academic Press, New York, **1981**; b) G. J. Meyer, *Molecular Level Artificial Photosynthetic Materials*, Wiley, New York, **1997**.

[9] a) Q. Xie, E. Perz-Cordero, L. Echegoyen, *J. Am. Chem. Soc.* **1992**, *114*, 3978–3980; b) H. Imahori, K. Tamaki, D. M. Guldi, C. Luo, M. Fujitsuka, O. Ito, Y. Sakata, S. Fukuzumi, *J. Am. Chem. Soc.* **2001**, *123*, 2607–2617.

[10] F. D'Souza, G. R. Deviprasad, M. E. Zandler, V. T. Hoang, A. Klykov, M. VanStipdonk, A. Perera, M. E. El-Khouly, M. Fujitsuka, O. Ito, *J. Phys. Chem. A* **2002**, *106*, 3243–3252.

[11] J. R. Lakowicz, *Principles of Fluorescence Spectroscopy*, 3rd ed., Springer, Singapore, **2006**.

[12] D. Rehm, A. Weller, *Isr. J. Chem.* **1970**, *8*, 259–271.

[13] The free-energy change for charge separation (ΔG_{CS}) from the singlet excited state $^1(F_{15}P)Zn^*$ within the donor–acceptor system is calculated using spectroscopic, computational, and electrochemical data following Equations (1)–(3).

$$-\Delta G_{CR} = E_{ox} - E_{red} + \Delta G_S \quad (1)$$

$$-\Delta G_{CS} = \Delta E_{0,0} - (-\Delta G_{CR}) \quad (2)$$

where $\Delta E_{0,0}$ and ΔG_{CS} correspond to the energy of excited singlet state and electrostatic energy, respectively. The E_{ox} and E_{red} represent the oxidation potential of the electron donor, $(F_{15}P)Zn$ and the reduction potential of the electron acceptors, C_{60}), respectively. The term ΔG_S refers to the static Coulombic energy, calculated by using the "dielectric continuum model" according to Equation (3):

$$\Delta G_s = e^2/4\pi\varepsilon_0 \left[\left(\tfrac{1}{2}R_+ + \tfrac{1}{2}R_- \right) \Delta(1/\varepsilon_R) - \tfrac{1}{R_{CC}\varepsilon_R} \right] \quad (3)$$

The symbols ε_0, and ε_R represent vacuum permittivity and dielectric constant of the solvent used for photochemical and electrochemical studies, respectively. R_{CC} is the center-to-center distance between donor and acceptor entities. The symbols R_+ and R_- refer to radii of the cation and anion species, respectively. The calculated ΔG_S was found to be 0.07 eV for the present donor–acceptor system.

[14] $k_{CS} = 1/\tau_{(F15P)Zn\text{-}C60} - 1/\tau_{(F15P)Zn}$, where $\tau_{(F15P)Zn\text{-}C60}$ and $\tau_{(F15P)Zn}$ refer to decay time constant of the dyad and control, respectively.

[15] Φ_f ($= [1/\tau_{(F15P)Zn\text{-}C60} - 1/\tau_{(F15P)Zn}]/1/\tau_{(F15P)Zn\text{-}C60}$), for abbreviations, see Ref. [14].